Compliance Control and Unstructured Modeling of Cooperating Robots

H. Kazerooni
T. I. Tsay

Mechanical Engineering Department
University of Minnesota
Minneapolis, Minnesota, 55455

Abstract

The work presented here is the description of the control strategy of two cooperating robots. A two-fingered hand is an example of such a system. We propose a control architecture that guarantees: 1) each robot end-point follows its position input command vector "closely" when the robots are not in contact with each other, and 2) when the two robots come in contact with each other, one robot controls the position of the contact point, while the other controls the contact force. The controller does not need any hardware or software switch for the transition between unconstrained and constrained maneuvering of each robot.

Introduction

This paper develops the essential rules in stability analysis of two cooperating robots. We assume the robots initially have some type of independent tracking capabilities. This assumption permits us to extend the control analysis to cover industrial robot manipulators in addition to research robots. The tracking capability allows each robot to follow its individual command independently when it is not constrained by each other. Once the robots come in contact with each other, the contact force between the two robots is fed back to one of the robots to develop compliancy (1,2,3,4). The compliancy in one of the robots allows for control of the contact force, while the other robot governs the position of the contact point. A stability bound has been developed on the size of the force feedback gain to stabilize the closed loop system of both robots. The stability analysis has been investigated using unstructured models for the dynamic behavior of the robot manipulators. This unified approach of modeling robot dynamics is expressed in terms of sensitivity functions as opposed to the Lagrangian approach. It allows us to incorporate the dynamic behavior of all the elements of a robot manipulator (i.e. actuators, sensors and the structural compliance of the links) in addition to the rigid body dynamics(4).

Dynamic Model of the Robot

In this section, a general approach will be developed to describe the dynamic behavior of a large class of industrial and research robot manipulators having positioning (tracking) controllers. The fact that most industrial manipulators already have some kind of positioning controller is the motivation behind our approach. Also, a number of methodologies exist for the development of robust positioning controllers for direct and non-direct robot manipulators (6).

In general, the end-point position of a robot manipulator that has a positioning controller is a dynamic function of its input trajectory vector, e, and the external force, f. (f is measured in the global coordinate frame also.) Let G and S be two L_p stable mappings that describe the robot end-point position, y, in a global coordinate frame.

$$y = G(e) + S(f) \qquad (1)$$

The assumption that linear superposition (in equation 1) holds for the effects of f and e is useful in understanding the nature of the interaction between two robots. This interaction is in a feedback form and will be clarified with the help of Figure 1. We will note later that the results of the nonlinear analysis do not depend on this assumption, and one can extend the obtained results to cover the case when G(e) and S(f) do not superimpose. The motion of the robot end-point in response to imposed forces, f, is caused either by structural compliance in the robot[1] or by the compliance of the positioning controller. Robots with tracking controllers are not infinitely stiff in response to external forces (also called disturbances). Even though the positioning controllers of robots are usually designed to follow the trajectory commands and reject disturbances, the robot end-point will move somewhat in response to imposed forces on it. S is called the sensitivity function and it maps the external force to the robot end-point position. For a robot with a "good" positioning controller, S is a mapping with small gain. No assumption on the internal structures of G(e) and S(f) is made. We define S^{-1} as inverse function of the S function:

$$f = S^{-1}[y - G(e)] \qquad (2)$$

Dynamics of Two Robots

Suppose two manipulators with dynamic equation 1 are in contact with each other. Equations 3 and 4 represent the entire dynamic behavior of two interacting robots.

$$y_1 = G_1(e_1) + S_1(f_1) \qquad (3)$$

$$f_2 = S_2^{-1}[y_2 - G_2(e_2)] \qquad (4)$$

where: $y_1 = y_2$ and $f_1 = -f_2$

Figure 1 shows the block diagram of the interaction of two robots. Note that the blocks in Figure 1 are in general non-linear operators, however, in the linear case one can treat these blocks as transfer function matrices.

---

[1] In a simple example , if a Remote Center Compliance (RCC) with a linear dynamic behavior is installed at the end-point of the robot, then S is equal to the reciprocal of stiffness (impedance in the dynamic sense) of the RCC.
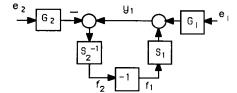
Figure 1: Interaction of Two Robots

If all the operators of the block diagram in Figure 1 were transfer function matrices, then the contact force, f_2, could be calculated from equation 5.

$$f_2 = (S_1 + S_2)^{-1}(G_1 e_1 - G_2 e_2) \tag{5}$$

Equation 5 motivates the block diagram of Figure 2 for representation of the contact force in the system where V_1 and V_2 are given by equations 6 and 7.

$$V_1 = (S_1 + S_2)^{-1} G_1 \tag{6}$$

$$V_2 = (S_1 + S_2)^{-1} G_2 \tag{7}$$
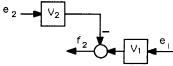
$$f_2 = V_1 e_1 - V_2 e_2 \tag{8}$$

Figure 2: V_1 and V_2 describe the contributions of both inputs, e_1 and e_2.

We assume Figure 2 is valid for representation of the non-linear case also. In other words, considering equations 3 and 4 as original equations for dynamic behavior of the robots, one can arrive at operators V_1 and V_2 to show the contributions of e_1 and e_2 on the contact force. We assume V_1 and V_2 are two L_p-stable operators, in other words $V_1(e_1)$: $L_p^n \mapsto L_p^n$ and $V_2(e_2)$: $L_p^n \mapsto L_p^n$ and also there exsit positive scalars α_1, α_2, β_1 and β_2 such that:

$$\|V_1(e_1)\|_p \leqslant \alpha_1 \|e_1\|_p + \beta_1 \tag{9}$$

$$\|V_2(e_2)\|_p \leqslant \alpha_2 \|e_2\|_p + \beta_2 \tag{10}$$

See Appendix A for some definitions on the L_p stability.

The Closed-loop System for Two Robots

The control architecture in Figure 3 shows how we develop compliancy in the system. H_2 is a compensator to be designed for the second robot. The input to this compensator is the contact force, f_2. The compensator output signal is being added vectorially with the input command vector, r_2, resulting in the error signal, e_2 for the second robot manipulator. One can think of this architecture as a system that allows the second robot to "control" the force and the first robot to "control" the position.

There are two feedback loops in the system; the first loop (which is the natural feedback loop), is the same as the one shown in Figure 1. This loop shows how the contact force affects the robots in a natural way when two robots are in contact with each other. The second feedback loop is the controlled feedback loop.

If two robots are not in contact, then the dynamic behavior of each robot reduces to the one represented by equation 1, which is a simple tracking system. When the robots are in contact with each other, then the contact forces and the
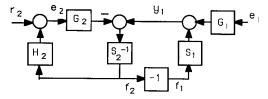

Figure 3: The Closed-loop System , the first robot controls the position and the second robot controls the force.

end-point positions of robots are given by f_1, f_2, y_1 and y_2 where the following equations are true:

$$y_1 = G_1(e_1) + S_1(f_1) \tag{11}$$

$$f_2 = S_2^{-1}(y_2 - G_2(e_2)) \tag{12}$$

$$y_1 = y_2 \tag{13}$$

$$f_1 + f_2 = 0 \tag{14}$$

$$e_2 = r_2 + H_2(f_2) \tag{15}$$

If all the operators are considered linear transfer function matrices, then[2]:

$$f_2 = (S_1 + S_2 + G_2 H_2)^{-1}(G_1 e_1 - G_2 r_2) \tag{16}$$

We plan to choose a class of compensators, H_2, to control the contact force with the input command r_2. This controller must also guarantee the stability of the closed-loop system shown in Figure 3. When two robots are not in contact with each other, the actual end-point position of each robot is almost equal to its input trajectory command governed by equation 1. When the robots are in contact with each other, the contact force on the second robot follows r_2 according to equations 11-15. The input command vector, r_2, is used differently for the two categories of maneuverings of the second robot; as an input trajectory command in unconstrained space (equation 1) and as a command to control force in constrained space.

Stability

The objective of this section is to arrive at a sufficient condition for stability of the system shown in Figures 3. This sufficient condition leads to the introduction of a class of compensators, H_2, that can be used to develop compliancy for the class of robot manipulators that have positioning controllers. The following theorem (Small Gain Theorem) (7,8) states the stability condition of the closed-loop system shown in Figure 4. A corollary is given to represent the size of H_2 to guarantee the stability of the system.
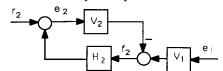

Figure 4: Two Manipulators with Force Feedback Compensator.

If conditions I, II and III hold:

I. V_1 and V_2 are L_p- stable operators, that is $V_1(e_1)$: $L_p^n \mapsto L_p^n$

---

[2]Note that the robot sensitivity functions and the electronic compliancy , $G_2 H_2$, add together to form the total sensitivity of the system. If $H_2 = 0$, then only the sensitivity functions of two robots add together to form the compliancy for the system. By closing the loop via H_2, one can not only add to the total sesitivity but also shape the sensitivity of the system.

and $V_2(e_2)$: $L^n_p \mapsto L^n_p$ and:

a) $\quad \| V_1(e_1) \|_p \leqslant \alpha_1 \| e_1 \|_p + \beta_1$ (17)

b) $\quad \| V_2(e_2) \|_p \leqslant \alpha_2 \| e_2 \|_p + \beta_2$ (18)

II. H_2 is chosen such that mapping $H_2(f_2)$ is L_p-stable, that is

a) $\quad H_2(f_2)$: $L^n_p \mapsto L^n_p$ (19)

b) $\quad \| H_2(f_2) \|_p \leqslant \alpha_3 \| f \|_p + \beta_3$ (20)

III.   and $\alpha_2 \alpha_3 < 1$ (21)

then the closed loop system in Figure 4 is stable. The proof is given in Appendix A. The following corollary develops a stability bound if H_2 is selected as a linear transfer function matrix.

Corollary

The key parameter in the proposition is the size of $\alpha_2 \alpha_3$. According to the proposition, to guarantee the stability of the system, H_2 must be chosen such that $\alpha_2 \alpha_3 < 1$. If H_2 is chosen as a linear operator (the impulse response) while all the other operators are still nonlinear, then:

$$\| H_2 (f_2) \|_p \leqslant \gamma \| f_2 \|_p \quad\quad\quad (22)$$

where : $\quad \gamma = \sigma_{max} (N)$ (23)

σ_{max}[3] indicates the maximum singular value, and N is a matrix whose ijth entry is $\| H_{ij} \|_1$. In other words, each member of N is the L_1 norm of each corresponding member of H_2. Considering inequality 22, the third stability condition, inequality 21, can be rewritten as:

$$\gamma \alpha_2 < 1 \quad\quad\quad (24)$$

To guarantee the closed loop stability, $\gamma \alpha_2$ must be smaller than unity, or, equivalently:

$$\gamma < \frac{1}{\alpha_2} \quad\quad\quad (25)$$

To guarantee the stability of the closed loop system, H_2 must be chosen such its "size" is smaller than the reciprocal of the "gain" of the forward loop mapping in Figure 4. Note that γ represents a "size" of H_2 in the singular value sense.

When all the operators are linear transfer function matrices one can use Multivariable Nyquist Criterion to arrive at the sufficient condition for stability of the closed loop system. This sufficient condition leads to the introduction of a class of transfer function matrices, H_2, that stabilize the family of linearly treated robot manipulators. The detailed derivation for the stability condition is given in Appendix B. Appendix C shows that the stability condition given by Nyquist Criterion is a subset of the condition given by the Small Gain Theorem. Using the results in Appendix B, the sufficient condition for stability is given by inequality 26.

$$\sigma_{max}(H_2) < \frac{1}{\sigma_{max}((S_1 + S_2)^{-1} G_2)} \quad \forall \omega \in (0, \infty) \quad (26)$$

Similar to the nonlinear case, H_2 must be chosen such that its "size" is smaller than the reciprocal of the "size" of the forward loop mapping in Figure 5 to guarantee the stability of the closed loop system. Note that in inequality 26 σ_{max} represents a "size" of H_2 in the singular value sense.

Consider n=1 (one degree of freedom system) for more understanding about the stability criterion. The stability criterion when n=1 is given by inequality 27.

---

[3]The maximum singular value of a matrix A, $\sigma_{max}(A)$ is defined as:

$$\sigma_{max}(A) = \max \frac{|A z|}{|z|}$$

where z is a non-zero vector and $|.|$ denotes the Euclidean norm.

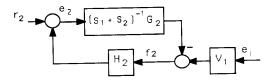**Figure 5:** In the Linear Case, $V_2 = (S_1 + S_2)^{-1} G_2$ and $V_1 = (S_1 + S_2)^{-1} G_1$

$$|G_2 H_2| < |(S_1 + S_2)| \quad\quad \forall \omega \in (0, \infty) \quad (27)$$

where $|\cdot|$ denotes the magnitude of a transfer function. Since in many cases $G_2 \approx 1$ within the bandwidth of the tracking controller of each robot, ω_0, then H_2 must be chosen such that:

$$|H_2| < |S_1 + S_2| \quad\quad \forall \omega \in (0, \omega_0) \quad (28)$$

Inequality 28 reveals some facts about the size of H_2. The smaller the sensitivity functions of the robot manipulators are, the smaller H_2 must be chosen. In the "ideal case", no H_2 can be found to allow two perfect tracking robots $(S_1 = S_2 = 0)$ interact with each others. In other words, for the stability of the system shown in Figure 3, there must be some compliancy in either first or second robot. RCC, structural dynamics and the tracking controller stiffness form the compliancy on the robot.

Suppose, the first robot is an ideal positioning system. In other words, S_1 has a zero gain. Therefore the contact force and the position of contact point between two robots are:

$$f_{2\infty} = (S_2 + G_2 H_2)^{-1} (G_1 e_1 - G_2 r_2) \quad (29)$$

$$y_{1\infty} = G_1(e_1) \quad\quad\quad (30)$$

The first robot controls the position of the contact point, while the other controls the contact force. Generalizing this concept to n robots, one robot controls the position of the contact point while the other robots control the n-1 contact forces such that :

$$f_1 + f_2 + f_3 + \ldots + f_n = 0 \quad\quad\quad (31)$$

Summary and Conclusion

A new architecture for compliance control of two cooperating robots has been investigated using unstructured models for dynamic behavior of robots. Each robot end-point follows its position input command vector "closely" when the robots are not in contact with each other. When two robots come in contact with each other, one robot controls the position of the contact point, while the other controls the contact force. The unified approach of modeling robots is expressed in terms of sensitivity functions. A bound for the global stability of the manipulators has been derived. For the stability of two robots, there must be some initial compliancy in either robot. The initial compliancy in the robots can be obtained by a non-zero sensitivity function for the tracking controller or a passive compliant element such as an RCC.

Example

Consider two one-degree of freedom robots with G and S in equation 1 given as:

$$G_1(s) = \frac{0.85}{(s/5 + 1)(s/9 + 1)(s/190 + 1)(s/240 + 1)(s/290 + 1)}$$

$$S_1(s) = \frac{0.1}{(s/4 + 1)(s/8 + 1)}$$

$$G_2(s) = \frac{1}{(s/6 + 1)(s/10 + 1)(s/200 + 1)(s/250 + 1)(s/300 + 1)}$$

$$S_2(s) = \frac{0.05}{(s/5 + 1)(s/9 + 1)}$$

Both robots have good positioning capability (small gain for S). The poles that are located at -250, -300, -290, -240 show the high frequency modes in the robots. The stability of the robots when they are in contact with each other is analyzed. If we consider H_2 as a constant gain, then inequality 27 yields that for $H_2 < 0.08$ the value of $|G_2H_2|$ is always smaller than $|S_1 + S_2|$ for all $\omega \in (0,\infty)$. Figure 6 shows the plots of $|G_2H_2|$ and $|S_1 + S_2|$ for three values of H_2. For $H_2 = 0.05$ the system is stable with the closed loop poles located at (-456.71, -147.24 ± 172.37J, -9.41, -8.38, -5.62, -4.58) while $H_2 = 1$ results in unstable system with the closed loop poles located at (-800.88, -9.03, -8.05, -5.05, -4.13, 23.98 ± 474.35J). Note that the stability condition derived via inequality 27 is a sufficient condition for stability; many compensators can be found to stabilize the system without satisfying inequality 27. Figure 6 shows an example ($H_2 = 0.25$) that does not satisfy inequality 27 however the system is stable with closed loop poles at (-598.64, -76.87 ± 298.04J, -9.1, -8.15, -5.19, -4.36). If one uses root locus for stability analysis, for $H_2 < 0.75$ all the closed loop poles will be in the left half plane. Once a constant value for stabilizing H_2 established, one can choose a dynamic compensator to filter out the high frequency noise in the force measurements.

$$H_2 = \frac{0.05}{.1s + 1}$$

a: $|G_2H_2|$, $H_2 = 1$
b: $|G_2H_2|$, $H_2 = 0.25$
c: $|G_2H_2|$, $H_2 = 0.05$
d: $|S_1 + S_2|$

Figure 6: $|G_2H_2| < |S_1 + S_2|$ is a sufficient condition for stability.

Appendix A

Definitions 1 to 7 will be used in the stability proof of the closed-loop system (7,8).

Definition 1: For all $p \in (1, \infty)$, we label as L^n_p the set consisting of all functions $f = [f_1, f_2, ..., f_n]^T$: $(0, \infty) \mapsto \mathbb{R}^n$ such that:

$$\int_0^\infty |f_i|^p \, dt < \infty \qquad \text{for} \quad i = 1, 2, ..., n$$

Definition 2: For all $T \in (0, \infty)$, the function f_T defined by:

$$f_T = \begin{cases} f & 0 < t < T \\ 0 & T < t \end{cases}$$

is called the truncation of f to the interval $(0, T)$.

Definition 3: The set of all functions $f = [f_1, f_2, ..., f_n]^T$:

$(0, \infty) \mapsto \mathbb{R}^n$ such that $f^T \in L^n_p$ for all finite T is denoted by L^n_{pe}. f by itself may or may not belong to L^n_p.

Definition 4: The norm on L^n_p is defined by:

$$\|f\|_p = \left[\sum_{i=1}^n \|f_i\|_p^2 \right]^{1/2}$$

where $\|f_i\|_p$ is defined as:

$$\|f_i\|_p = \left[\int_0^\infty w_i |f_i|^p \, dt \right]^{1/p}$$

where w_i is the weighting factor. w_i is particularly useful for scaling forces and torques of different units.

Definition 5: Let $V_2(\cdot): L^n_{pe} \mapsto L^n_{pe}$. We say that the operator $V_2(\cdot)$ is L_p- stable, if:

a) $V_2(\cdot): L^n_p \mapsto L^n_p$

b) there exist finite real constants α_2 and β_2 such that:

$$\|V_2(e_2)\|_p \leq \alpha_2 \|e_2\|_p + \beta_2 \qquad \forall \, e_2 \in L^n_p$$

According to this definition we first assume that the operator maps L^n_{pe} to L^n_{pe}. It is clear that if one does not show that $V_2(\cdot): L^n_{pe} \mapsto L^n_{pe}$, the satisfaction of condition (a) is impossible since L^n_{pe} contains L^n_p. Once the mapping of $V_2(\cdot)$ from L^n_{pe} to L^n_{pe} is established, then we say that the operator $V_2(\cdot)$ is L_p-stable if whenever the input belongs to L^n_p the resulting output belongs to L^n_p. Moreover, the norm of the output is not larger than α_2 times the norm of the input plus the offset constant β_2.

Definition 6: The smallest α_2 such that there exists a β_2 so that inequality b of Definition 5 is satisfied is called the gain of the operator $V_2(\cdot)$.

Definition 7: Let $V_2(\cdot): L^n_{pe} \mapsto L^n_{pe}$. The operator $V_2(\cdot)$ is said to be causal if:

$$V_2(e_2)_T = V_2(e_{2T}) \quad \forall T < \infty \qquad \text{and} \qquad \forall \, e_2 \in L^n_{pe}$$

Proof of the nonlinear stability proposition

Define the closed-loop mapping $A:(e_1, r_2) \mapsto e_2$ (Figure 4).

$$e_2 = r_2 + H_2 [V_1(e_1) - V_2(e_2)] \tag{A1}$$

For each finite T, inequality A2 is true.

$$\|e_{2T}\|_p \leq \|r_{2T}\|_p + \|H_2[V_1(e_1) - V_2(e_2)]_T\|_p \quad \forall T < \infty \tag{A2}$$

$H_2[V_1(e_1) - V_2(e_2)]$ is L_p- stable, therefore, using inequalities 17, 18, and 20:

$$\|e_{2T}\|_p \leq \|r_{2T}\|_p + \alpha_3 \alpha_1 \|e_{1T}\|_p + \alpha_3 \alpha_2 \|e_{2T}\|_p + \alpha_3 \beta_1 + \alpha_3 \beta_2 + \beta_3 \quad \forall T < \infty \tag{A3}$$

Since $\alpha_3 \alpha_2$ is less than unity:

$$\| e_{2T} \|_p \leq \frac{\| e_{1T} \|_p}{1 - \alpha_3 \alpha_2} + \frac{\| r_{2T} \|_p}{1 - \alpha_3 \alpha_2}$$

$$+ \frac{\alpha_3 (\beta_1 + \beta_2) + \beta_3}{1 - \alpha_3 \alpha_2} \quad \forall T < \infty \qquad (A4)$$

Inequality A4 shows that $e_2(.)$ is bounded over $[0,T]$. Because this reasoning is valid for every finite T, it follows that $e_2(.) \in L^n_{pe}$, i.e., that $A:L^n_{pe} \to L^n_{pe}$. Next we show that the mapping A is L_p-stable in the sense of definition 5. Since $\| r_2 \|_p$ and $\| e_1 \|_p < \infty$ (they both belong to L^n_p space), then from inequality A4:

$$\| e_{2T} \|_p < \infty \qquad \forall T < \infty \qquad (A5)$$

In the limit when $T \to \infty$:

$$\| e_2 \|_p < \infty \qquad (A6)$$

Inequality A6 implies e_2 belongs to L^n_p -space whenever r_2 and e_1 belong to L^n_p- space. With the same reasoning from equations A1 to A5, it can be shown that inequality A7 is true.

$$\| e_2 \|_p \leq \frac{\| e_1 \|_p}{1 - \alpha_3 \alpha_2} + \frac{\| r_2 \|_p}{1 - \alpha_3 \alpha_2}$$

$$+ \frac{\alpha_3 (\beta_1 + \beta_2) + \beta_3}{1 - \alpha_3 \alpha_2} \qquad (A7)$$

Inequality A7 shows the linear boundedness of e_2. (Condition b of definition 5) Inequality A7 and A6 taken together, guarantee that the closed-loop mapping A is L_p-stable.

Appendix B

The objective is to find a sufficient condition for stability of the closed-loop system in Figure 5 by Nyquist Criterion. The block diagram in Figure 5 can be reduced to the block diagram in Figure B1 when all the operators are linear transfer function matrices.
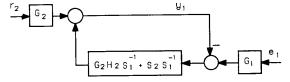

Figure B1: Simplified Block-Diagram of the System in Figure 5

There are two elements in the feedback loop; $G_2 H_2 S_1^{-1}$ and $S_2 S_1^{-1}$. $S_2 S_1^{-1}$ shows the natural force feedback while $G_2 H_2 S_1^{-1}$ represents the controlled force feedback in the system. The objective is to use Nyquist Criterion (5) to arrive at the sufficient condition for stability of the system when $H_2 = 0$. The following conditions are regarded:

1) The closed loop system in Figure B1 is stable if $H_2 = 0$. This condition simply states the stability of two robot manipulators. (Figure 2 shows this configuration.)
2) H_2 is chosen as a stable linear transfer function matrix. Therefore the augmented loop transfer function $[G_2 H_2 S_1^{-1} + S_2 S_1^{-1}]$ has the same number of unstable poles that $S_2 S_1^{-1}$ has. Note that in many cases $S_2 S_1^{-1}$ is a stable system.
3) Number of poles on $j\omega$ axis for both loop $S_2 S_1^{-1}$ and $[G_2 H_2 S_1^{-1} + S_2 S_1^{-1}]$ are equal.

Considering that the system in Figure B1 is stable when $H_2 = 0$, we plan to find how robust the system is when $G_2 H_2 S_1^{-1}$ is added to the feedback loop. If the loop transfer function

$S_2 S_1^{-1}$ (without compensator, H_2) develops a stable closed-loop system, then we are looking for a condition on H_2 such that the augmented loop transfer function $[G_2 H_2 S_1^{-1} + S_2 S_1^{-1}]$ guarantees the stability of the closed-loop system. According to the Nyquist Criterion, the system in Figure B1 remains stable if the anti-clockwise encirclement of the $\det(G_2 H_2 S_1^{-1} + S_2 S_1^{-1} + I_n)$ around the center of the s-plane is equal to the number of unstable poles of the loop transfer function $[G_2 H_2 S_1^{-1} + S_2 S_1^{-1}]$. According to conditions 2 and 3, the loop transfer functions $S_2 S_1^{-1}$ and $[G_2 H_2 S_1^{-1} + S_2 S_1^{-1}]$ both have the same number of unstable poles. The closed-loop system when $H_2 = 0$ is stable according to condition 1; the encirclements of $\det(S_2 S_1^{-1} + I_n)$ is equal to unstable poles of $S_2 S_1^{-1}$. Since the number of unstable poles of $[G_2 H_2 S_1^{-1} + S_2 S_1^{-1}]$ and that of $S_2 S_1^{-1}$ are the same, therefore for stability of the system $\det(G_2 H_2 S_1^{-1} + S_2 S_1^{-1} + I_n)$ must have the same number of encirclements that $\det(S_2 S_1^{-1} + I_n)$ has. A sufficient condition to guarantee the equality of the number of encirclements of $\det(G_2 H_2 S_1^{-1} + S_2 S_1^{-1} + I_n)$ and that of $\det(S_2 S_1^{-1} + I_n)$ is that the $\det(G_2 H_2 S_1^{-1} + S_2 S_1^{-1} + I_n)$ does not pass through the origin of the s-plane for all possible non-zero but finite values of H_2, or

$$\det(G_2 H_2 S_1^{-1} + S_2 S_1^{-1} + I_n) = 0 \quad \forall \omega \in (0, \infty) \quad (B1)$$

If inequality B1 does not hold then there must be a non-zero vector z such that:

$$(G_2 H_2 S_1^{-1} + S_2 S_1^{-1} + I_n) z = 0 \qquad (B2)$$

$$\text{or}: \quad G_2 H_2 S_1^{-1} z = - (S_2 S_1^{-1} + I_n) z \qquad (B3)$$

A sufficient condition to guarantee that equality B3 will not happen is given by inequality B4.

$$\sigma_{max} (G_2 H_2 S_1^{-1}) < \sigma_{min} (S_2 S_1^{-1} + I_n) \ \forall \omega \in (0, \infty) \quad (B4)$$

or a more conservative condition:

$$\sigma_{max} (H_2) < \frac{1}{\sigma_{max}[(S_1 + S_2)^{-1} G_2]} \quad \forall \omega \in (0, \infty) \quad (B5)$$

Note that $[S_1 + S_2]^{-1} G_2$ is the transfer function matrix that maps e_2 to the contact force, f_2 when $e_1 = 0$. Figure 5 shows the closed-loop system. According to the result of the proposition, H_2 must be chosen such that the size of H_2 is smaller than the reciprocal of the size of the forward loop transfer function, $(S_1 + S_2)^{-1} G_2$.

Appendix C

The following inequalities are true when $p = 2$ and H_2 and V_2 are linear operators.

$$\| H_2(f_2) \|_p \leq \gamma \| f_2 \|_p \qquad (C1)$$

$$\| V_2(e_2) \|_p \leq \mu \| e_2 \|_p \qquad (C2)$$

where:

$\mu = \sigma_{max}(Q)$, and Q is the matrix whose ijth entry is given by $[Q]_{ij} = \sup_\omega |[V_2]_{ij}|$,

$\nu = \sigma_{max}(R)$, and R is the matrix whose ijth entry is given by $[R]_{ij} = \sup_\omega |[H_2]_{ij}|$

According to the stability condition, to guarantee the closed loop stability $\mu \nu < 1$ or:

$$\nu < \frac{1}{\mu} \qquad\qquad\qquad\qquad \text{(C3)}$$

Note that the following are true:

$$\sigma_{max}(V_2) \leqslant \mu \qquad \forall \omega \in [0, \infty) \qquad \text{(C4)}$$

$$\sigma_{max}(H_2) \leqslant \nu \qquad \forall \omega \in [0, \infty) \qquad \text{(C5)}$$

Substituting C4 and C5 into inequality C3 which guarantees the stability of the system, the following inequality is obtained:

$$\sigma_{max}(H_2) < \frac{1}{\sigma_{max}(V_2)} \qquad \forall \omega \in [0,\infty) \qquad \text{(C6)}$$

$$\sigma_{max}(H_2) < \frac{1}{\sigma_{max}((S_1+S_2)^{-1} G_2)} \quad \forall \omega \in [0,\infty) \quad \text{(C7)}$$

Inequality C7 is identical to inequality 26. This shows that the linear stability condition by the multivariable Nyquist Criterion is a subset of the general condition given by the Small Gain Theorem.

References

1) Kazerooni, H. "Fundamentals of Robust Compliant Motion for Manipulators", IEEE Journal of Robotics and Automation , N2, V2, June 1986b.

2) Kazerooni, H, "A Design Method for Robust Compliant Motion of Manipulators", IEEE Journal of Robotics and Automation, N2, V2, June 1986c.

3) Kazerooni, H., Guo, J., "Design and Construction of an Active End-Effector", In proceedings of the IEEE International Conference on Robotics and Automation, Raleigh, North Carolina, April 1987, and also IEEE Journal of Robotics and Automation.

4) Kazerooni, H, "On the Stability of the Robot Compliant Motion Control, "In proceedings of the IEEE CDC, Dec. 87.

5) Lehtomaki, N. A., Sandell, N. R., Athans, M., "Robustness Results in Linear-Quadratic Gaussian Based Multivariable Control Designs", IEEE Transaction on Automatic Control AC-26(1):75-92, February, 1981.

6) Spong, M. W., Vidyasagar, M., "Robust Nonlinear Control of Robot Manipulators", IEEE Conference on Decision and Control", December 1985.

7) Vidyasagar, M., "Nonlinear Systems Analysis", Prentice-Hall, 1978.

8) Vidyasagar, M., Desoer, C. A., "Feedback Systems: Input-Output Properties", Academic Press, 1975.